Journal of Modern Physics, 2019, 10, 91-101
http://www.scirp.org/journal/jmp
ISSN Online: 2153-120X
ISSN Print: 2153-1196

Structure and Photoluminescence Properties of Pr^{3+} Ion-Doped BaY_2ZnO_5 Phosphor Prepared Using a Sol-Gel Method

Hung-Rung Shih[1], Mu-Tsun Tsai[2], Lay-Gaik Teoh[3], Yee-Shin Chang[4*]

[1]Department of Mechanical and Computer-Aided Engineering, National Formosa University, Taiwan
[2]Department of Materials Science and Engineering, National Formosa University, Taiwan
[3]Department of Mechanical Engineering, National Pingtung University of Science and Technology, Taiwan
[4]Department of Electronic Engineering, National Formosa University, Taiwan
Email: *yeeshin@nfu.edu.tw

How to cite this paper: Shih, H.-R., Tsai, M.-T., Teoh, L.-G. and Chang, Y.-S. (2019) Structure and Photoluminescence Properties of Pr^{3+} Ion-Doped BaY_2ZnO_5 Phosphor Prepared Using a Sol-Gel Method. *Journal of Modern Physics*, **10**, 91-101.
https://doi.org/10.4236/jmp.2019.102008

Received: January 7, 2019
Accepted: February 9, 2019
Published: February 12, 2019

Copyright © 2019 by author(s) and Scientific Research Publishing Inc.
This work is licensed under the Creative Commons Attribution International License (CC BY 4.0).
http://creativecommons.org/licenses/by/4.0/
Open Access

Abstract

The Pr^{3+} ion-doped BaY_2ZnO_5 phosphor with the orthorhombic structure was synthesized successfully using a sol-gel method in this study. The SEM images show that the BaY_2ZnO_5:Pr^{3+} phosphor particles are aggregational but have an isotropic distribution for 2 mol% Pr^{3+} ions doped. Under an excitation wavelength of 311 nm, the emission bands that appear in the emission spectra are due to the $^3P_0 \rightarrow {}^3H_{4,5,6}$, $^1D_2 \rightarrow {}^3H_4$ and $^3P_0 \rightarrow {}^3F_2$ electron transition of Pr^{3+} ion, and it is the same as that for solid state reaction preparation. Comparing to the solid state reaction preparation, the intensities of the $^3P_0 \rightarrow {}^3H_4$ transition were increased by about 6.5 times for sol-gel method. The enhancement in emission intensity is because the activators have more homogeneous contribution in host for the sol-gel method preparation. In addition, the color tone did not change very obviously, which located around the green light region for Pr^{3+} ion concentrations increasing. The color stability is better for sol-gel method than that for the solid state reaction preparation.

Keywords

Phosphor, Rare Earth Oxides, Optical Properties

1. Introduction

Oxide phosphors have recently gained much attention for applications such as screens infield-emission displays (FEDs) [1], plasma display panels (PDPs) [2] [3] and for white color light-emitting diodes (LEDs) [4] because the intrinsic problems such as their higher chemical stability and resistance to moisture rela-

tive to that of traditional phosphors are rare earth or transition metal activated sulphides such as ZnS, SrS, and CaS. A lot of efforts have been done to discover the novel host materials as well as activators with high photoluminescence properties including emission intensity, high quantum yield and so on for phosphor applications [5] [6].

The emission of lanthanide ion, Pr^{3+} ion, in the visible region occurs because of the transition of the $^3P_0$ level, which contains two dominant transitions from the fluorescent $^3P_0$ level to the lower $^3H_6$ and $^3H_4$ states [7]. The emission spectra of Pr^{3+} are significantly different in different hosts and can take the form of red, green, or even blue emissions [8] [9].

BaY_2ZnO_5 has the orthorhombic structure with space of Pbnm [10], and it consists of YO_7, BaO_{11}, and ZnO_5 polyhedra. BaY_2ZnO_5 is an excellent host for various activator ions-doped phosphors. Some previous studies investigated the effect of the size, morphology of particles, and activator concentrations on the photoluminescence properties of BaY_2ZnO_5:RE^{3+} phosphors [11] [12] [13] [14]. According to our previous study [14], the emission spectra show that the $^3P_0 \rightarrow {}^3H_{4,5,6}$ transitions are dominant for the Pr^{3+}-doped BaY_2ZnO_5 phosphor. The color tone changes from green to greenish and finally yellow, as the Pr^{3+} ion concentration increases.

Many efforts have been done to enhance the emission intensities of phosphors and the improvement of particle morphologies via fluxes addition, chemical methods utilized to mix activators well or by doping with ions of different radii. Various chemical methods have been investigated for synthesizing fine-sized grains, because these have been reported to enhance the emission efficiency and intensity of phosphors [15] [16]. These methods include sol-gel [17] [18] [19], hydrothermal [20] [21] [22], and precipitate techniques [23]. Among these methods, the sol-gel process is an attractive route that starts from molecular precursors and forms an oxide network via inorganic polymerization reactions, and offers both product and processing advantages, such as high purity, ultrahomogeneity, and reduction of the calcining temperature, which could decrease the grain size and enhance the emission efficiency and intensity of phosphors.

In this investigation, the Pr^{3+} ions-doped BaY_2ZnO_5 phosphor was prepared using a sol-gel method to reduce the preparation parameters, improve the surface morphology, and hope to increase to the luminescence efficiency of phosphor. The influences of Pr^{3+} ion concentrations on the resulting structure and the photoluminescence (PL) properties of BaY_2ZnO_5:Pr^{3+} phosphor were also studied. The results indicated that the calcination conditions are lower than that of the solid state reaction, and the intensities of emission peak increased by about 6.5 times for the sol-gel method.

2. Experimental Procedure

In this study, BaY_2ZnO_5 compounds doped with various concentrations of Pr^{3+} ions were synthesized using a sol-gel method. The raw materials of barium ni-

tride [$Ba(NO_3)_2$], yttrium acetate [$Y(OOCCH_3)_3 \cdot 4H_2O$], zinc acetate [$Zn(OOCCH_3)_2$] and praseodymium acetate [$Pr(OOCCH_3)_3 \cdot xH_2O$] with a purity of 99.99% were supplied by Alfa Aesar. At the first, barium nitride (0.01 mole), zinc acetate (0.01 mole), yttrium acetate (0.02 - 2x mole) and praseodymium acetate (2x mole, x = 0 - 0.005) were separately dissolved in 100 ml of deionized water, respectively. Secondly, barium nitride, zinc acetate, yttrium acetate and praseodymium acetate solutions were mixed in a round bottom flask. When the precursor was completely dissolved in the solution, predetermined amounts of citric acid and ethylene glycol (equal molar ratio) were added to the solution mentioned above as a chelating agent and stabilizing agent, respectively. The amounts of citric acid and ethylene glycol were determined by the ratio of citric acid to metal cations. At last, the powders obtained were calcined in air at 1200˚C for 6 h.

Characterization

Powders were analyzed for crystal structure by X-ray diffractometry (XRD; Rigaku Dmax-33 x-ray diffractometer, Tokyo, Japan) using Cu-Karadiation with a source power of 30 kV and a current of 20 mA to identify the possible phases formed after heat treatment. The surface morphologies of phosphors were examined using high resolution scanning electron microscopy (HR-SEM, S4200, Hitachi). Optical absorption spectra were measured at room temperature using a Hitachi U-3010 UV-vis spectrophotometer. Both the excitation and emission spectra of the phosphors were measured using a Hitachi F-7000 fluorescence spectrophotometer with a 150 W xenon arc lamp as the excitation source at room temperature.

3. Results and Discussion

3.1. Structures

Figure 1 shows the X-ray diffraction patterns of the $Ba(Y_{1-x}Pr_x)_2ZnO_5$(x = 0 - 0.05) powders calcined in air at 1200˚C for 6 h. The XRD results show that all of the diffraction peaks of the $BaY_2ZnO_5:Pr^{3+}$ phosphors can be attributed to the orthorhombic structure (JCPDS 89-5856) for Pr^{3+} ion concentration from 0 to 5 mol%, and there is no second phase appears in the spectra, which demonstrates that the Pr^{3+} ion substitutes the Y^{3+} ion. The calcination conditions are lower than that of 1250˚C/12h for conventional ceramics processing reported by the solid state reaction [14]. When the Pr^{3+} content is further increased, the intensities of the diffraction peaks seem to be decrease, and the diffraction peak of the (131) shift to a lower diffraction angle. The shift of the peak position is $\Delta\theta$ = 0.68˚ for the Pr^{3+} ion concentration is 0 and 5 mol%. It is due to the Pr^{3+} ion (0.99 Å, 6-coordinated) has a larger radius than that of Y^{3+} ion (0.90 Å, 6-coordinated), the lattice distorts and intra-stress occurs, nonuniform strain in the vicinity of the Pr^{3+} ions is induced when a trivalent praseodymium ion is introduced to replace trivalent yttrium ion in the $BaY_2ZnO_5:Pr^{3+}$ system.

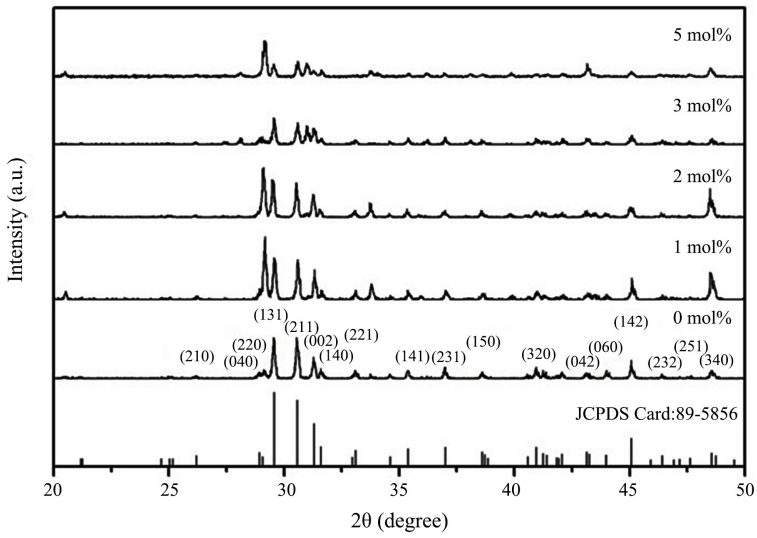

Figure 1. The X-ray diffraction patterns for different concentration of Pr^{3+} ion-doped BaY_2ZnO_5 phosphors prepared using sol-gel method.

Table 1 is the grain size calculated using the Scherrer's equation for different concentrations of Pr^{3+} ion-doped BaY_2ZnO_5 phosphor. The grain sizes for BaY_2ZnO_5:Pr^{3+} phosphors are all in the nanoscale range, and increase initially then decrease for Pr^{3+} ion concentration increase further. The largest grain size occurs when Pr^{3+} ion concentration is 2 mol%. The results are in good accordance with the analysis of XRD patterns for the intensity of (131) diffraction peak is increase then decrease as the Pr^{3+} ion concentration increases.

3.2. Microstructures

The size of phosphor particles should be as homogeneous as possible without any aggregates or agglomerates. Moreover, the surface of the phosphor particles should also be as smooth as possible and have a high degree of crystallization to improve efficiency. **Figure 2** shows the FE-SEM surface morphology of BaY_2ZnO_5 doped with 0, 1, 2, and 5 mol% Pr^{3+} ions. By the results, most of these phosphor particles have polyhedral shapes and irregular. These particles are agglomerates of smaller particles during the calcination process due to that they are on the nano-scale with large surface energies when the particles produced using this sol-gel method. When the Pr^{3+} ion concentration doping is 2 mol% (**Figure 2(c)**), the particles seem to be more uniform distribution and regular sizes. These phosphor powders with better surface morphologies will display a preferable photoluminescence property, and it will be good accordance with the optical properties measurement.

Figure 3 shows the absorption spectra of the BaY_2ZnO_5 doped with different Pr^{3+} ion concentrations phosphor calcined at 1200˚C in air for 6 h. For the host material, it shows two absorption broads in the UV region. The strong absorption band in the region from 200 to 270 nm is attributed to the band-to-band transitions, whereas the weaker broad band from 270 to 400 nm can be attri-

buted to the tightly bound Frankel excitons, which are usually observed close to the bandgap in large-bandgap crystals [24] [25]. The absorption edge of the BaY_2ZnO_5 host is located at ~378 nm. When Pr^{3+} ion doped, a stronger broad band in the range of 250 - 350 nm and a series of small peaks between 400 and 500 nm appear in the spectrum, and that are associated with the f-f transition of the Pr^{3+} ion. The stronger broad band centered at 311 nm can be attributed to the 4f - 5d characteristics transition absorption of Pr^{3+} ion. According to the studies [26] [27] [28], the typical Pr^{3+}-activated oxide phosphors always demonstrate strong 4f - 5d transition band absorption at approximately 200 - 330 nm, and it is in accordance with the results for our study. In addition, there also appears a series of absorption peaks from 440 to 500 nm and 580 to 620 nm, this can be attributed to the 4f orbital characteristics transition for the $^3H_4 \rightarrow {}^3P_J$ (J = 0, 1, 2) transition of the Pr^{3+} ion.

Table 1. The grain Size of $Ba(Y_{1-x}Pr_x)_2ZnO_5$(x = 0 - 0.05) phosphor calculated using the Scherrer's equation.

Pr^{3+}ion concentration	D_g (nm)
0	45.21
1	56.11
2	77.48
3	67.80
5	58.11

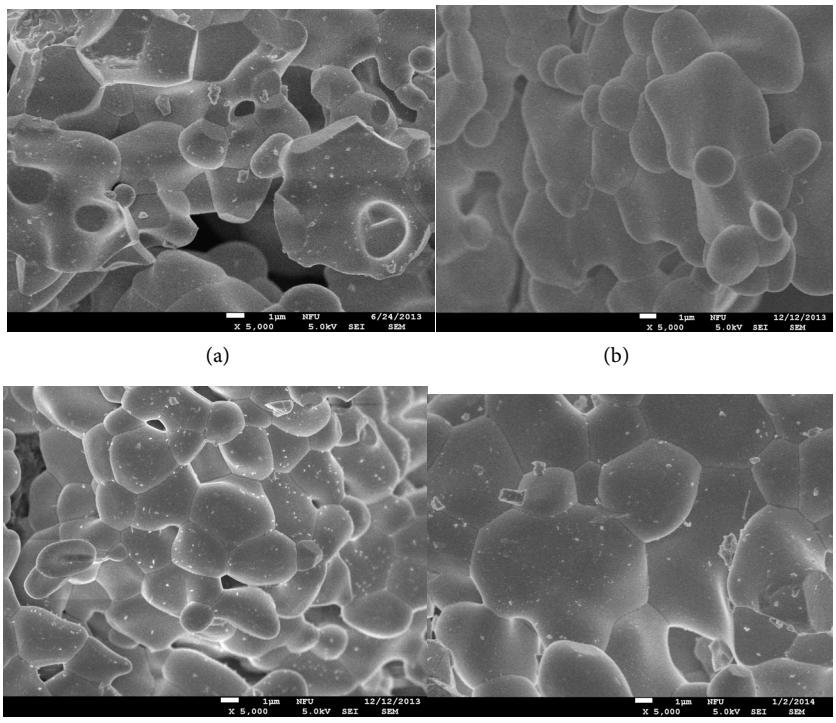

Figure 2. The FE-SEM micrographs of BaY_2ZnO_5 doped with different Pr^{3+} ion concentrations: (a) 0, (b) 1, (c) 2 and (d) 5 mol%.

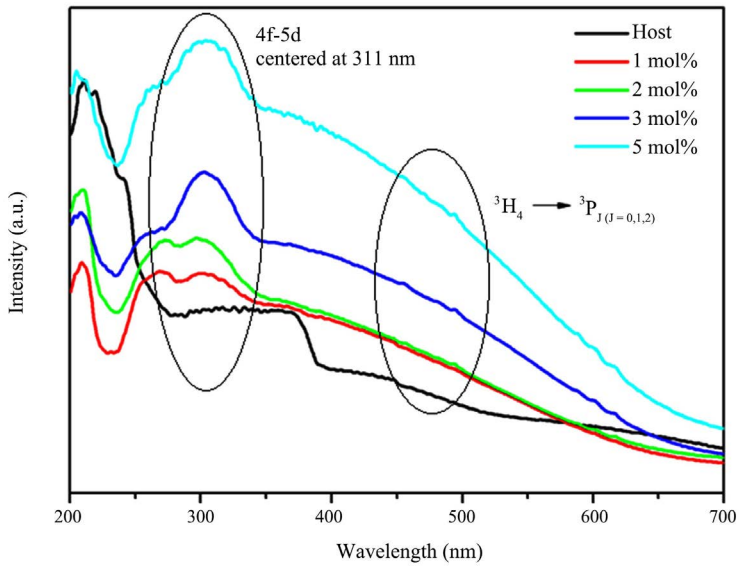

Figure 3. The absorption spectra of BaY_2ZnO_5 doped with different Pr^{3+} ion phosphor prepared using sol-gel method.

Figure 4(a) shows the excitation spectra for BaY_2ZnO_5 doped with various Pr^{3+} ion concentrations calcined in air at 1200˚C for 6 h using the sol-gel method, the singles were obtained by monitoring the emission wavelength of 513 nm for the $^3P_0 \rightarrow {}^3H_4$ transition. A strong broad band from 250 - 350 nm and some sharp peaks in the longer wavelength region can be observed in the excitation spectra. It is similar to the results observed in the absorption spectra, the 4f - 5d transition of Pr^{3+} ion centered at 311 nm was located in the broad band region. These sharp peaks centered at 458 nm, 485 nm and 495 nm in the longer wavelength region from 450 to 500 nm can be assigned to the f-f transitions of Pr^{3+} ion for the $^3H_4 \rightarrow {}^3P_2$, $^3H_4 \rightarrow {}^3P_1$ and $^3H_4 \rightarrow {}^3P_0$, transition, respectively [29] [30]. The excitation intensity has a maximum value for Pr^{3+} ion 2 mol% doped, and then decreasing as the Pr^{3+} ion concentration increases which is due to concentration quenching effect.

Figure 4(b) is the comparison for excitation spectra of BaY_2ZnO_5:2mol%Pr^{3+} phosphor synthesized using the solid state reaction and sol-gel method. As can be seen, different synthesization did not change the shape of excitation curve but did change the intensities of the excitation peak. The excitation intensity of 4f - 5d transition for BaY_2ZnO_5:2mol%Pr^{3+} phosphor synthesized by the sol-gel method is 1.5 times higher than that for the solid state reaction. In Addition, The peak of the 4f - 5d transition shifts from 315 (solid state reaction) to 311 nm (sol-gel method). This shift was associated with the size of the BaY_2ZnO_5:2mol%Pr^{3+} phosphors. It is caused by BaY_2ZnO_5:2mol%Pr^{3+} phosphor prepared using a sol-gel method (calcination at 1200˚C) with a smaller particle sizes then that for solid state reaction (calcination at 1250˚C). According to the studies [31], for a smaller particle size, lattice parameters were usually smaller than those of the bigger one because of the huge surface stress, which leads a stronger ligands field and hence the blue shift was often observed.

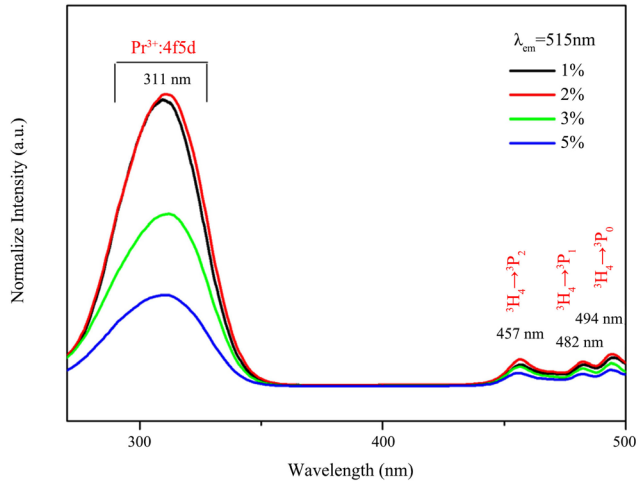

(a)

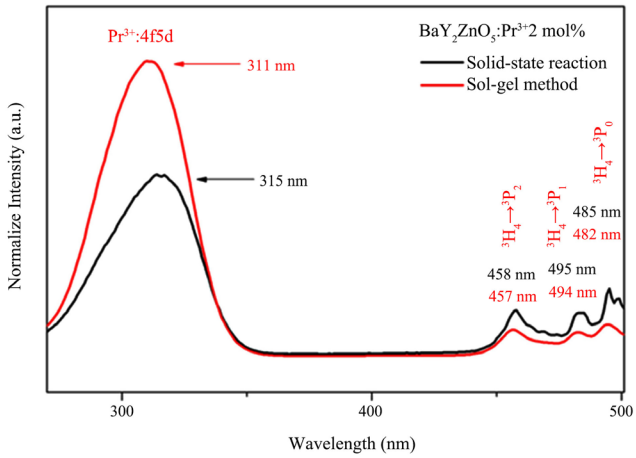

(b)

Figure 4. The excitation spectra of BaY_2ZnO_5 doped with different Pr^{3+} ion phosphor prepared using soli-gel method, and (b) the comparison of excitation spectra for BaY_2ZnO_5:2mol%Pr^{3+} phosphor prepared using sol-gel method and solid state reaction.

Figure 5(a) is the emission spectra under an excitation of 311 nm for BaY_2ZnO_5 doped with various Pr^{3+} ion concentrations prepared using the sol-gel method, and **Figure 4(b)** is the comparison of the emission spectra for BaY_2ZnO_5 doped with 2 mol% Pr^{3+} ions prepared by the solid state reaction and sol-gel method. As can be seen in **Figure 5(a)**, there are several light emitting peaks in the visible light ranges for 490 - 520 nm, and 530 - 560 nm, respectively. The emission peaks at 496, 499 and 515 nm are assigned to the $^3P_0 \rightarrow {}^3H_4$ transitions, those at 530, 539 and 555 nm are the $^3P_0 \rightarrow {}^3H_5$ transitions. It reached a maximum when the Pr^{3+} concentration was 2 mol%, and decreased with the increasing Pr^{3+} concentration, which indicated that the concentration quenching is active when $x > 0.02$. Comparison to the solid state reaction (**Figure 5(b)**), the intensities of the $^3P_0 \rightarrow {}^3H_4$ transition for BaY_2ZnO_5:2mol%Pr phosphor increased by about 6.5 times for sol-gel method. The enhancement in emission intensity is because the activators have more homogeneous contribution in host for the

sol-gel method preparation.

For $BaY_2ZnO_5:Pr^{3+}$ phosphor prepared using the sol-gel method, different concentrations of Pr^{3+} ion-doping has no effect on the wave shape, but did change the emission peaks intensities. The Commission Internationale de I'Eclairage (CIE) color coordinates of the different color tones for $Ba(Y_{1-x}Pr_x)ZnO_5$ phosphors prepared using the sol-gel method that are excited at 311 nm are shown in **Figure 6**. As the Pr^{3+} ion concentration increasing, the color tone did not change very obviously, and which located around the green light region. It possesses a better color stability for sol-gel method synthesization, because the color tone changes from green to greenish and finally to yellow light region as the Pr^{3+} ion concentrations increasing for solid state reaction preparation.

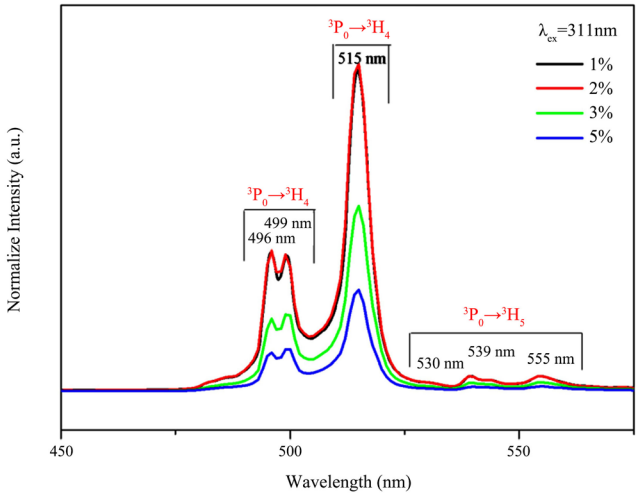

(a)

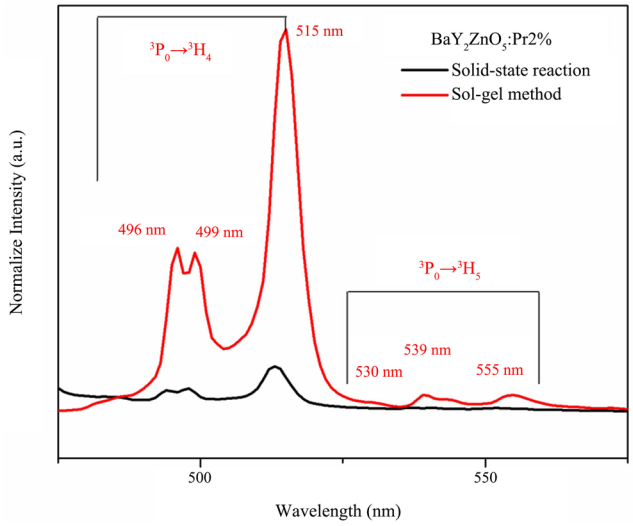

(b)

Figure 5. The emission spectra of BaY_2ZnO_5 doped with different Pr^{3+} ion phosphor prepared using soli-gel method, and (b) the comparison of excitation spectra for BaY_2ZnO_5:2mol%Pr^{3+} phosphor prepared using sol-gel method and solid state reaction.

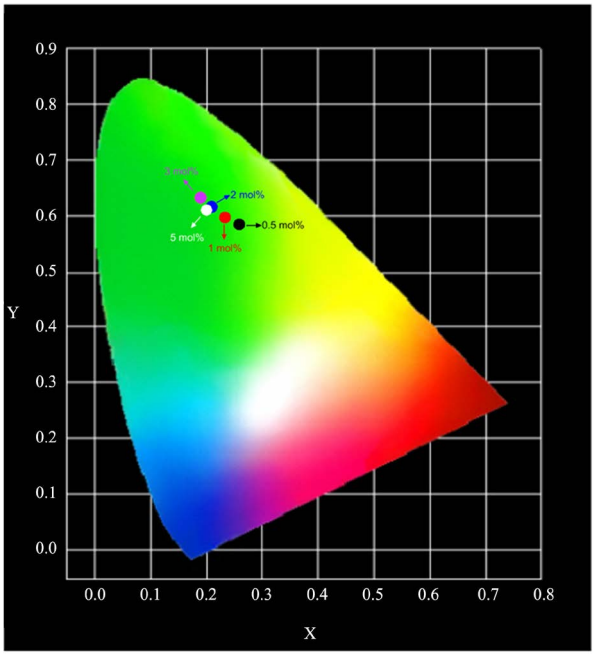

Figure 6. CIE chromaticity diagram for BaY_2ZnO_5 doped with various Pr^{3+} ion concentration.

4. Conclusion

In this study, the orthorhombic structure for Pr^{3+} ion-doped BaY_2ZnO_5 was synthesized successfully using a sol-gel method, and the calcination conditions are lower than that for the conventional ceramics processing. The SEM images show that the BaY_2ZnO_5:Pr^{3+} phosphor particles are aggregational but have an isotropic distribution for 2 mol% Pr^{3+} ions doped. Under an excitation wavelength of 311 nm, the emission bands that appear in the emission spectra are due to the $^3P_0 \rightarrow {}^3H_{4,5,6}$, $^1D_2 \rightarrow {}^3H_4$ and $^3P_0 \rightarrow {}^3F_2$ electron transition of Pr^{3+} ion, and it is the same as that for solid state reaction preparation. The optimum condition for Pr^{3+} ion concentration doped is 2 mol%, and the intensities of the $^3P_0 \rightarrow {}^3H_4$ transition are increased by about 6.5 times for sol-gel method. The enhancement in emission intensity is because the activators have more homogeneous contribution in host for the sol-gel method preparation. In addition, the color tone did not change very obviously, which located around the green light region for Pr^{3+}ion concentrations increasing. The color stability is better for sol-gel method than that for solid state reaction preparation.

Acknowledgements

The authors would like to thank the Ministry of Science and Technology of the Republic of China for financially supporting this project under grant MOST 107-2622-E-150-005-CC3.

Conflicts of Interest

The authors declare no conflicts of interest regarding the publication of this paper.

References

[1] Hsu, W.T., Wu, W.H. and Lu, C.H. (2003) *Materials Science and Engineering*: *B*, **104**, 40-44. https://doi.org/10.1016/S0921-5107(03)00268-X

[2] Mauch, R.H. (1996) *Applied Surface Science*, **92**, 589-597. https://doi.org/10.1016/0169-4332(95)00301-0

[3] Yi, L., Hou, Y., Zhao, H., He, D., Xu, Z., Wang, Y. and Xu, X. (2000) *Displays*, **21**, 147-149. https://doi.org/10.1016/S0141-9382(00)00046-9

[4] Zhao, X., Wang, X., Chen, B., Meng, Q., Di, W., Ren, G. and Yang, Y. (2007) *Journal of Alloys and Compounds*, **433**, 352-355. https://doi.org/10.1016/j.jallcom.2006.06.096

[5] Wakefield, G., Keron, H.A., Dobson, P.J. and Hutchison, J.L. (1999) *Journal of Colloid and Interface Science*, **215**, 179-182. https://doi.org/10.1006/jcis.1999.6225

[6] Jung, H.K., Park, D.S. and Park, Y.C. (1999) *Materials Research Bulletin*, **34**, 43-51. https://doi.org/10.1016/S0025-5408(98)00216-5

[7] Pedrini, C., Bouttet, D., Dujardin, C., Moine, B., Dafinei, I., Lecoq, P., Koselja, M. and Blazek, K. (1994) *Optical Materials*, **3**, 81-88. https://doi.org/10.1016/0925-3467(94)90010-8

[8] Piper, W., DeLuca, J. and Ham, F. (1974) *Journal of Luminescence*, **8**, 344-348. https://doi.org/10.1016/0022-2313(74)90007-6

[9] Sommerdijk, J., Bril, A. and De Jager, A. (1974) *Journal of Luminescence*, **8**, 341-343. https://doi.org/10.1016/0022-2313(74)90006-4

[10] Kaduk, J.A., Wing, N.W., Greenwood, W., Dillingham, J. and Toby, B.H. (1999) *Journal of Research of the National Institute of Standards and Technology*, **104**, 147-171. https://doi.org/10.6028/jres.104.011

[11] Liang, C.H., Chang, Y.C. and Chang, Y.S. (2008) *Applied Physics Letters*, **93**, Article ID: 211902. https://doi.org/10.1063/1.2998299

[12] Liang, C.H., Teoh, L.G., Liu, K.T. and Chang, Y.S. (2012) *Journal of Alloys and Compounds*, **517**, 9-13. https://doi.org/10.1016/j.jallcom.2011.11.088

[13] Shih, H.R. and Chang, Y.S. (2017) *Journal of Electronic Materials*, **46**, 6603-6608. https://doi.org/10.1007/s11664-017-5717-0

[14] Shih, H.R., Tsai, Y.Y., Liu, K.T., Liao, Y.Z. and Chang, Y.S. (2013) *Optical Materials*, **35**, 2654-2657. https://doi.org/10.1016/j.optmat.2013.08.007

[15] Shih, H.R., Tsai, M.T., Chen, H.L., Xiang, Y.X. and Chang, Y.S. (2014) *Materials Research Bulletin*, **55**, 33-37.

[16] Williams, D.K., Bihari, B., Tissue, B.M. and McHale, J.M. (1998) *The Journal of Physical Chemistry B*, **102**, 916-920.

[17] Zhang, J., Zhang, Z., Tang, Z., Lin, Y. and Zheng, Z. (2002) *Journal of Materials Processing Technology*, **121**, 265-268.

[18] Li, Y., Duan, X., Liao, H. and Qian, Y. (1998) *Chemistry of Materials*, **10**, 17-18.

[19] Hirano, M. (2000) *Journal of Materials Chemistry*, **10**, 469-472.

[20] Hirano, M., Imai, M. and Inagaki, M. (2000) *Journal of the American Ceramic Society*, **83**, 977-979. https://doi.org/10.1111/j.1151-2916.2000.tb01310.x

[21] Tas, A.C., Majewski, P.J. and Aldinger, F. (2002) *Journal of Materials Research*, **17**, 1425-1433.

[22] Nedelec, J.M., Mansuy, C. and Mahiou, R. (2003) *Journal of Molecular Structure*, **651-653**, 165-170.

[23] Li, J. and Kuwabara, M. (2003) *Science and Technology of Advanced Materials*, **4**, 143-148.

[24] Hashizume, K., Matsubayashi, M., Vachal, M. and Tani, T. (2002) *Journal of Luminescence*, **98**, 49. https://doi.org/10.1016/S0022-2313(02)00251-X

[25] Liang, C.H., Qi, X.D. and Chang, Y.S. (2010) *Journal of the Electrochemical Society*, **157**, 1169.

[26] Hoefdraad, H.E. and Blasse, G. (1975) *Physica Status Solidi* (*A*), **29**, K95-K97.

[27] Donega, C.D.M., Meijerink, A. and Blasse, G. (1995) *Journal of Physics and Chemistry of Solids*, **56**, 673-685.

[28] Dorenbos, P. (2000) *Journal of Luminescence*, **91**, 91. https://doi.org/10.1016/S0022-2313(00)00197-6

[29] Lin, Y.F., Chang, Y.H., Chang, Y.S., Tsai, B.S. and Li, Y.C. (2006) *Journal of the Electrochemical Society*, **153**, G543.

[30] Raju, G.S.R., Park, J.Y., Jung, H.C., Balarkrishnaiah, R., Moon, B.K. and Jeong, J.H. (2011) *Current Applied Physics*, **11**, S292-S295.

[31] Huang, S.C., Wu, J.K., Hsu, W.J., Chang, H.H., Hung, H.Y., Lin, C.L., Su, H.Y., Bagkar, N., Ke, W.C., Kuo, H.T. and Liu, R.S. (2009) *International Journal of Applied Ceramic Technology*, **6**, 465.